


# Outcomes of Spatially Fractionated Radiotherapy (GRID) for Bulky Soft Tissue Sarcomas in a Large Animal Model

Technology in Cancer Research & Treatment  
2017, Vol. 16(3) 357–365  
© The Author(s) 2017  
Reprints and permission:  
sagepub.com/journalsPermissions.nav  
DOI: 10.1177/1533034617690980  
journals.sagepub.com/home/tct  


Michael W. Nolan, DVM, PhD<sup>1,2</sup>, Tracy L. Gieger, DVM<sup>1,2</sup>,  
Alexander A. Karakashian, PhD<sup>3</sup>, Mariana N. Nikolova-Karakashian, PhD<sup>3</sup>,  
Lysa P. Posner, DVM<sup>4</sup>, Donald M. Roback, PhD<sup>5</sup>, Judith N. Rivera, MS<sup>6</sup>,  
and Sha Chang, PhD<sup>1,6,7,8</sup>

## Abstract

GRID directs alternating regions of high- and low-dose radiation at tumors. A large animal model mimicking the geometries of human treatments is needed to complement existing rodent systems (eg, microbeam) and clarify the physical and biological attributes of GRID. A pilot study was undertaken in pet dogs with spontaneous soft tissue sarcomas to characterize responses to GRID. Subjects were treated with either 20 Gy (3 dogs) or 25 Gy (3 dogs), delivered using 6 MV X-rays and a commercial GRID collimator. Acute toxicity and tumor responses were assessed 2, 4, and 6 weeks later. Acute Radiation Therapy Oncology Group grade I skin toxicity was observed in 3 of the 6 dogs; none experienced a measurable response, per Response Evaluation Criteria in Solid Tumors. Serum vascular endothelial growth factor, tumor necrosis factor  $\alpha$ , and secretory sphingomyelinase were assayed at baseline, 1, 4, 24, and 48 hours after treatment. There was a trend toward platelet-corrected serum vascular endothelial growth factor concentration being lower 1 and 48 hours after GRID than at baseline. There was a significant decrease in secretory sphingomyelinase activity 48 hours after 25 Gy GRID ( $P = .03$ ). Serum tumor necrosis factor  $\alpha$  was quantified measurable at baseline in 4 of the 6 dogs and decreased in each of those subjects at all post-GRID time points. The new information generated by this study includes the observation that high-dose, single fraction application of GRID does not induce measurable reduction in volume of canine soft tissue sarcomas. In contrast to previously published data, these data suggest that GRID may be associated with at least short-term reduction in serum concentration of vascular endothelial growth factor and serum activity of secretory sphingomyelinase. Because GRID can be applied safely, and these tumors can be subsequently surgically resected as part of routine veterinary care, pet dogs with sarcomas are an appealing model for studying the radiobiologic responses to spatially fractionated radiotherapy.

## Keywords

canine, microenvironment, ablative, endothelial, abscopal

<sup>1</sup> Department of Clinical Sciences, College of Veterinary Medicine, North Carolina State University, Raleigh, NC, USA

<sup>2</sup> Comparative Medicine Institute, North Carolina State University, Raleigh, NC, USA

<sup>3</sup> Department of Physiology, College of Medicine, University of Kentucky, Lexington, KY, USA

<sup>4</sup> Department of Molecular and Biomedical Sciences, College of Veterinary Medicine, North Carolina State University, Raleigh, NC, USA

<sup>5</sup> Department of Radiation Oncology, Rex Cancer Center, Raleigh, NC, USA

<sup>6</sup> Department of Radiation Oncology, University of North Carolina, Chapel Hill, NC, USA

<sup>7</sup> Department of Physics and Astronomy, University of North Carolina, Chapel Hill, NC, USA

<sup>8</sup> Joint Department of Biomedical Engineering, University of North Carolina and North Carolina State University, Chapel Hill, NC, USA

## Corresponding Author:

Michael W. Nolan, DVM, PhD, Department of Clinical Sciences, College of Veterinary Medicine, North Carolina State University, 1052 William Moore Drive, Raleigh, NC 27607, USA.

Email: mwnolan@ncsu.edu



## Abbreviations

CT, computed tomography; IV, intravenous; MU, motor unit; PTV, planning target volume; RECIST, Response Evaluation Criteria in Solid Tumors; RT, radiation therapy; RTOG, Radiation Therapy Oncology Group; S-SMase, secretory sphingomyelinase; STS, soft tissue sarcoma; SFRT, spatially fractionated radiation therapy; TNF, tumor necrosis factor; VEGF, vascular endothelial growth factor

Received: September 02, 2016; Revised: December 07, 2016; Accepted: January 03, 2017.

## Introduction

Spatially fractionated radiation therapy (SFRT) involves intentional direction of highly nonuniform radiation fluences toward tumors. The first reports of SFRT describe passing orthovoltage X-ray beams through sieve-like collimators; orthovoltage radiation is poorly penetrating, so the goal of this so-called GRID therapy was to improve dose deposition in deep-seated tumors, while maintaining acceptable normal tissue complication rates in superficial tissues (eg, skin).<sup>1-3</sup> This approach became obsolete with the advent of megavoltage radiation therapy, which is both deeply penetrant and naturally skin sparing. There has, however, been a recent resurging interest in SFRT, fueled in part by clinical reports of positive outcomes for the management of bulky tumors in human patients with cancer treated with a combination of megavoltage GRID therapy and conventionally fractionated radiation therapy (RT).<sup>4-6</sup> Preclinical research has also shown that impressive normal tissue sparing can be achieved through delivery of microbeam radiation, a small-scale version of SFRT, as compared with confluent (broad-beam) radiation.<sup>7-10</sup> Finally, there are data suggesting the potential for SFRT to advantageously alter the tumor microenvironment, with regard to both immune and microvascular functions.<sup>11,12</sup>

Current clinical SFRT practice involves delivery of 10 to 20 Gy of GRID in a single fraction, followed by a course of conventionally fractionated radiation therapy. There have also been reports of using advanced radiotherapy planning and delivery techniques to create 3-dimensional SFRT that restricts the high-dose regions to occurring within tumors, while sparing surrounding normal tissues from unnecessary exposures; this technique is often referred to as LATTICE.<sup>13-15</sup> Regardless of the technical implementation (GRID or LATTICE), it is unclear why this approach of single fraction SFRT preceding conventional conformal irradiation has yielded impressive local tumor control in patients with bulky tumors, for which there would be a limited prognosis with conventional radiation therapy alone. It is also postulated that vascular, immunologic, and bystander effects may contribute to the clinical success of SFRT. Significant clinical- and laboratory-based efforts have supported the role of the tumor microenvironment in SFRT. For example, it has been shown that high-dose GRID results in acute induction of tumor necrosis factor  $\alpha$  (TNF- $\alpha$ ), ceramide, and secretory sphingomyelinase (S-SMase), which can be measured in serum of human patients with cancer and which

correlates strongly with the probability of a measurable tumor response.<sup>16,17</sup> Ceramide and S-SMase in particular have been proposed to enhance the direct effects of radiation on the tumor cells through their ability to induce apoptosis in the tumor microvascular endothelial cells.<sup>18</sup> In addition to these clinical investigations, a substantial body of work exists, wherein tumor and normal tissue responses to mini- and microbeam irradiation in mice have been studied.<sup>7-9,12</sup>

There are, however, significant limitations to the use of rodent models, largely related to the fact that the kilovoltage X-ray mini- and microbeam geometries do not reflect the physical characteristics of clinically utilized megavoltage SFRT approaches; these physical differences likely give rise to significant differences in biologic responses. A large animal model system would aid in overcoming some of these limitations and complement the available animal models. We therefore propose studying responses to SFRT in pet dogs with spontaneously occurring tumors. This model has the advantages of using SFRT beam geometries and tumor geometries, which closely mirror those encountered in human cancer clinics, as well as responses of tumors which can be studied in the setting of a naturally developing host tumor microenvironment, inclusive of an intact immune system. Another potential advantage of the proposed pet dog model is the ability to study the biologic effects of SFRT in tissue samples obtained when surgical removal of the tumor (as part of standard clinical management of veterinary patients) follows application of SFRT. Furthermore, it may also be possible to expand the utility of this pet dog "model" to allow the study of the short- and long-term impacts of SFRT *in situ*, if such treatment provides meaningful palliation for otherwise unresectable tumors. Through this pilot study, we therefore sought to characterize the clinical and biologic responses to high-dose, single fraction GRID therapy in pet dogs with spontaneously occurring soft tissue sarcomas (STS). We opted to focus on STS because these are common in pet dogs, are usually superficial, and thus accessible for repeated tissue sampling, and display similar clinical and biological features to the human condition. Canine STS are common on extremities and the trunk. They locally invade soft tissues. Metastasis does not occur frequently or early. Standard treatment for low- and intermediate-grade STS involves wide surgical excision. Postoperative, definitive-intent radiation therapy (an example of a common protocol being 3 Gy fractions, delivered daily [Monday through Friday] for a total of 18 fractions) is recommended when histologic margins are narrow

or incomplete.<sup>19</sup> Adjuvant chemotherapy is only considered for high-grade STS, where the metastatic rate is  $\sim 40\%$ . Radiotherapy can also be useful for the management of unresectable STS. Measurable responses (tumor volume reduction) are experienced by approximately 50% of patients, and the median progression-free interval is 1 year, when full-course radiotherapy (eg, 3 Gy  $\times$  18 fractions) is employed.<sup>20,21</sup> More commonly, hypofractionated radiotherapy is employed for the management of bulky STS in dogs, which controls tumors for approximately 6 months.<sup>22,23</sup> Recently, stereotactic body radiotherapy has been used for the management of unresectable canine STS. Results of early experiences have not yet been published, but in the experience of these authors, it is common to employ protocols such as 20 Gy  $\times$  1 fraction or 10 Gy  $\times$  3 fractions. Anecdotally, response rates and duration are similar to that reported for full-course radiotherapy. Colleagues at our institution have used canine STS as a comparative model for studying response to heat and radiotherapy for many years.<sup>20,24-29</sup>

## Materials and Methods

### Animals

A total of 6 privately owned pet dogs with spontaneously occurring STS were studied. Dogs were presented for evaluation at the College of Veterinary Medicine, North Carolina State University. This study was approved by the University's Institutional Animal Care and Use Committee (protocol identification 13-151-O).

Dogs were eligible for enrollment in this prospective clinical study if they had a histologically or cytologically confirmed STS that was at least 6 cm in diameter. Subjects had to be free of gross metastatic disease, as assessed by evaluation of the draining lymph node and thoracic radiography. Subjects also had to be free of concurrent illness, which would preclude general anesthesia. Subjects with ulcerated, or otherwise unhealthy, integument overlying the tumor were excluded. Study participation was offered to pet owners in cases where standard therapy was declined. Because the study was short in duration and focused on local tumor effects, complete clinical staging was not required. Because some dogs were enrolled with a cytologic diagnosis of STS, tumor grade was not known in all cases. Signed informed consent was obtained from all owners.

### GRID Therapy Dosimetry

GRID radiation is delivered using a commercial GRID collimator (Dot Decimal Inc, Sanford, Florida) placed on a standard linear accelerator (Novalis TX; Varian Medical Systems, Palo Alto, California). GRID therapy dosimetry is generally characterized by dose underneath one of collimator openings at the depth of  $D_{\max}$  (peak dose) and the dose between the adjacent collimator openings (valley dose).<sup>30</sup> The monitor unit (MU) per dose is calculated by the prescribed treatment dose divided by a GRID collimator factor. The GRID collimator factor is defined as the ratio of the peak dose using the GRID collimator at a

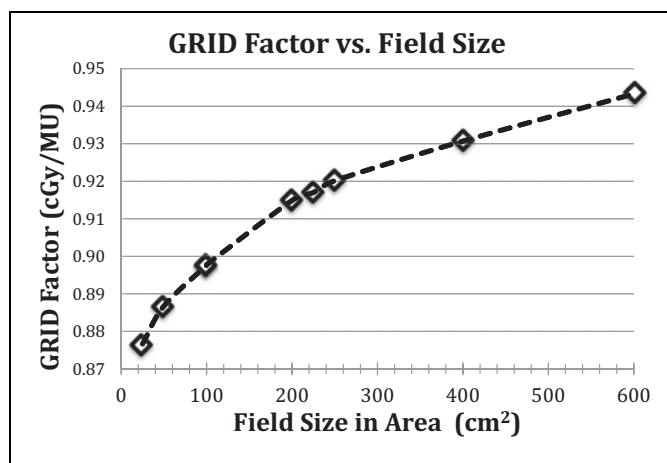


**Figure 1.** Measured GRID factor as a function of treatment field size (cm<sup>2</sup>) at isocenter ( $d = D_{\max}$ ) for 6 MV X-rays on a Novalis TX linear accelerator using a brass GRID collimator. For a given field size (in area) and GRID treatment dose, the monitor units are calculated using the GRID factor curve, above. We have explored different formats of GRID field factor as a function of treatment portal sizes, including equivalent square field size, and total area of the field size for a range of field sizes and shapes we anticipated to use for the GRID therapy in dogs. We found that the GRID factor and field size in area capture the most stable relationship, of all tested.

given field size and the dose under the accelerator output calibration condition, where 1 MU gives 1.0 cGy of dose. The GRID factor is a function of field size and photon energy (6 and 10 MV) is measured using an ion chamber (PTW 30013 Waterproof Farmer Chamber; RD Inc, Albertville, Minnesota) and Mapcheck QA device (Sun Nuclear Corp, Melbourne, Florida). The measured field size range is from 5 cm  $\times$  5 cm to 25 cm  $\times$  24 cm (maximum field size to be used with the GRID collimator). Figure 1 shows the dose per MU dependence on beam energy and field size for GRID therapy. Two-dimensional dose distribution at depth of  $D_{\max}$  is measured using RTQA2 GAFchromic film (Ashland Inc, Covington, Kentucky). Figures 2 and 3 show the GRID radiation beam profile and the percentage depth dose along the central axis of the beam, respectively.

### Treatment Planning and Irradiation

All subjects underwent general anesthesia for radiation therapy simulation using computed tomography (CT) and again 1 to 3 days later for GRID therapy. Computed tomography images were obtained before and after intravenous (IV) administration of an iodinated contrast medium (159.1 mg/kg iohexol, Omnipaque 350; GE Healthcare, Princeton, New Jersey). Organs at risk and targets were contoured on the simulation CT using a commercial treatment planning system (Eclipse version 11.0; Varian Medical Systems, Palo Alto, California). The planning target volume (PTV) was defined by a 1-cm isotropic expansion applied to the gross tumor volume. A single fraction of either 20 or 25 Gy was prescribed to a depth of 1.5 cm ( $D_{\max}$ ) and delivered through the GRID collimator. A single field, at

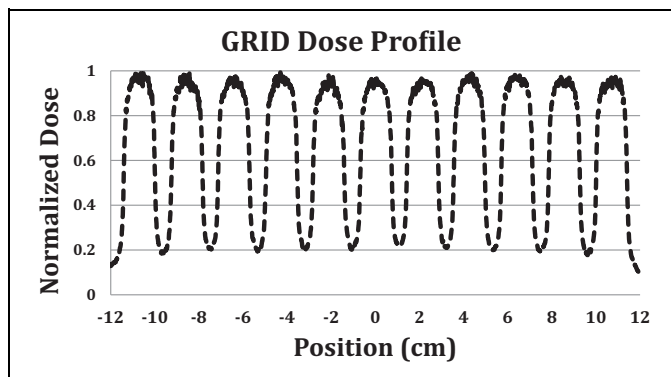


**Figure 2.** A 6-MV GRID field (25 cm × 24 cm) beam profile. The dose profile is measured at  $D_{\max}$  using Gafchromic RTQA-2 film. The film density is converted to dose using a film density calibration curve based on ion chamber data in conventional (non-GRID) fields.

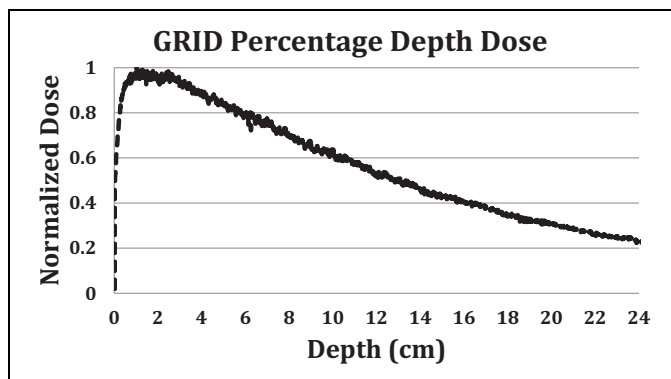


**Figure 3.** Percentage depth dose (PDD) of the 6-MV photon 15 cm × 15 cm GRID field, through the central opening of the GRID collimator. The GRID factor is defined as the ratio of dose at  $D_{\max}$  of a GRID field of given size and dose at  $D_{\max}$  of a 10 × 10 cm field under machine output calibration condition, times the machine output factor of 1 cGy/MU. We determined the relative dose ratio by measuring the dose on the central diode detector of a MapCHECK array system from a given GRID field radiation and a 10 × 10 cm field radiation under the same setup (100 cm SSD, central axis, with no additional build-up). We assumed that the depth difference between 6 MV  $D_{\max}$  (1.5 cm) and the measurement depth (2 cm) has negligible effect on the relative GRID factor measurement. SSD = Source to surface distance.

100 cm source-to-surface distance, was used and shaped to shield tissues outside the PTV using a multileaf collimator. No bolus was used. The MU calculation was computed based on the prescription dose and the GRID collimator factor for the chosen beam energy and field size. In all cases, treatment was delivered using a 6 MV X-ray beam. Monitor unit calculations were performed manually by the prescribing radiation oncologist and independently verified by a medical physicist. Appropriate patient and tumor positioning were verified immediately prior to treatment delivery, using kilovoltage cone-beam CT. The linear accelerator is designated for veterinary and research use only; the output calibration is performed based on the methodologies of AAPM TG-51; daily, monthly, and annual quality assurance testing is performed per American Association

of Physicists in Medicine, Task Group Report 142 (AAPM TG-142).

### Clinical Outcomes

Subjects were evaluated for radiation toxicity during recheck examination performed 2, 4, and 6 weeks after GRID irradiation, using Radiation Therapy Oncology Group (RTOG) acute radiation morbidity scoring criteria.<sup>31</sup> There is a published and peer-reviewed veterinary RTOG acute radiation morbidity scoring scheme.<sup>32</sup> However, this veterinary scheme is limited by lack of separation between what the RTOG classifies as grade 3 versus 4 toxicity and therefore is not directly translatable toxicity scoring in human trials. Therefore, to maximize translational potential, we directly applied the RTOG criteria to dogs, without modification. Tumor responses were also quantified via Response Evaluation Criteria in Solid Tumors (RECIST) at those visits.<sup>33</sup>

### Secondary End Points

Serum and plasma were obtained prior to and 1, 4, 24, and 48 hours after GRID irradiation; aliquots of each were stored at  $-80^{\circ}\text{C}$ . The S-SMase activity was measured using  $\text{C}_6$ -NBD-SM as a substrate in serum samples. The standardized assay contained 0.5  $\mu\text{L}$  serum, 20  $\mu\text{M}$  NBD-SM, 0.1 mM  $\text{ZnCl}_2$ , and 0.1 M sodium acetate buffer (pH 5.0) in a final volume of 20  $\mu\text{L}$ . Control assays contained 5 mM of EDTA instead of the  $\text{ZnCl}_2$ . Preliminary analyses determined the range of linearity of the assay with respect to the volume of serum used as an enzyme source. Reactions were allowed to continue for 3 hours at  $37^{\circ}\text{C}$  and were stopped by the addition of 0.5 mL methanol. After further incubation at  $37^{\circ}\text{C}$  for 30 minutes, the samples were centrifuged at 1000g and the generation of fluorescent product, NBD-ceramide was monitored by a reverse-phase high-pressure liquid chromatograph using methanol:water:phosphoric acid (850:150:0.15, by volume) as a mobile phase.<sup>34</sup> External standards were used to calculate the quantum yield of the NBD-SM and its product, NBD-ceramide. Specific activity was calculated as the difference in the activity measured in the presence of  $\text{Zn}^{2+}$  and EDTA and presented as nmol/mL/h. Materials for this assay included N-(6-((7-nitro-2-1,3-benzoxadiazol-4-yl)amino)hexanoyl)-*D*-erythro-sphingosine ( $\text{C}_6$ -NBD-Cer) and N-(6-((7-nitro-2-1,3-benzoxadiazol-4-yl)amino)hexanoyl)-sphingosine-1-phosphocholine ( $\text{C}_6$ -NBD-sphingomyelin) from Molecular Probes Inc (Eugene, Oregon). Tumor necrosis factor  $\alpha$  and vascular endothelial growth factor (VEGF) were quantified in serum using commercial assays (Canine TNF- $\alpha$  and VEGF Quantikine ELISA kits; R&D Systems, Inc, Minneapolis, Minnesota). Serum VEGF concentrations were corrected for platelet concentration.

### Statistical Analysis

Temporal changes in analyte concentrations were compared using Friedman nonparametric test for repeated measures. All

**Table 1.** Patient Demographics and Pretreatment Description of Tumors.

Subject ID	Signalment	Body Weight	Tumor Type	Maximum Tumor Diameter	Tumor Location
1	Castrated male, Maltese	4.85 kg	Soft tissue sarcoma, grade III	7.5 cm	Left antebrachium
2	Castrated male, Chow Chow	30.4 kg	Soft tissue sarcoma, grade III	9.8 cm	Left caudal thigh
3	Spayed female, Labrador retriever	28.7 kg	Chondrosarcoma	21 cm	Left lateral thorax
4	Spayed female, mixed breed	23.6 kg	Soft tissue sarcoma, grade I	22 cm	Left lateral thorax
5	Castrated male, American Eskimo	18.5 kg	Soft tissue sarcoma, grade III	11 cm	Right cranial thigh
6	Castrated male, American Staffordshire terrier	29.9 kg	Soft tissue sarcoma, grade I	7.5 cm	Left elbow

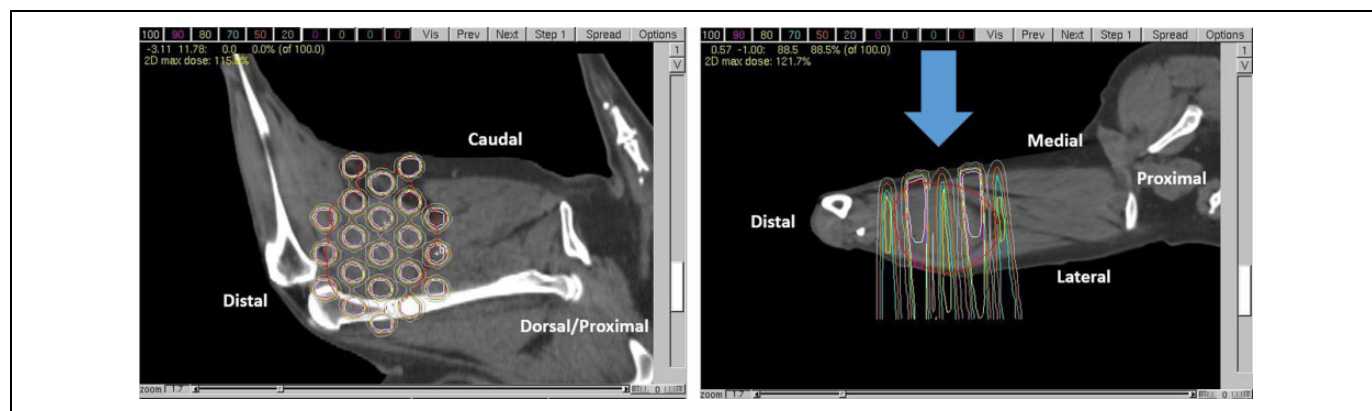


**Figure 4.** Example of a GRID treatment plan for the same dog that is shown in Figure 5. Dose is depicted via relative isodose lines on a parasagittal image (left: correlating with the beams-eye view) and an axial image (right) wherein the blue arrow indicates the beam’s axis; the tumor is located on the cuadolateral thigh, and anatomic orientation is provided (eg, caudal, distal). The gross tumor volume is outlined in red.

statistical tests were performed using commercial software (Prism version 6; GraphPad Software, Inc, La Jolla, California).

**Results**

Single fraction GRID therapy appears safe but does not result in a measurable tumor response in dogs with macroscopic STS. Six dogs were enrolled and treated with GRID alone, at 20 Gy (3 dogs) and 25 Gy (3 dogs). All subjects were 11 years old at the time of enrollment; other patient demographics data and pre-treatment tumor characteristics are summarized in Table 1. Based on tumor location and beam orientation for GRID treatments, skin was an important organ at risk to consider in evaluating for acute radiation toxicity. Aside from partial lung irradiation (~15% of total lung volume) in 2 subjects, exposure of visceral organs within the thoracic and abdominal cavities was completely avoidable. Figure 4 is an example of a GRID treatment plan for a canine sarcoma, demonstrating how the radiation dose maps onto the tumor volume. Clinically, dose calculation was performed via manual calculation of MUs, as described; this figure was a simulation generated using actual CT data from an enrolled subject (subject 2) and the University of North Carolina’s in-house treatment planning system, PLUNC.

**Table 2.** Treatment Descriptions and Oncologic Outcomes (Toxicity and Response).

Subject ID	GRID Dose (Gy)	Maximum RTOG Acute Toxicity Score	Objective Response 6 Weeks Post-GRID
1	20	0	Progressive disease
2	20	1	Stable disease
3	20	0	Not evaluable
4	25	0	Stable disease
5	25	1	Stable disease
6	25	1	Stable disease

Abbreviation: RTOG, Radiation Therapy Oncology Group.

Oncologic outcomes are summarized in Table 2. Briefly, 1 dog (subject 1) had its tumor surgically excised, 5 weeks post-GRID (20 Gy) due to progressive local tumor growth. Histopathology of the tumor confirmed a high-grade STS, with marked cortical and paracortical hyperplasia, but no evidence of metastasis in the draining lymph node. Surgical margins were free of neoplastic cells (wide margins); there were large areas of necrosis and inflammatory infiltrates (histiocytes, lymphocytes, and plasma cells), which are common in high-grade STS, but no specific pathologic changes that were attributable to GRID irradiation. Another dog (subject 3) was euthanized 3 weeks post-GRID (20 Gy) due to persistent and





**Figure 5.** Photograph of grade I skin toxicity (focal alopecia on the lateral aspect of the thigh, where the GRID collimated radiation exited the body).

poorly controlled tumor-associated pain. Autopsy was performed, and histopathologic evaluation of the tumor confirmed the mass to be a chondrosarcoma. There were regions of hemorrhage, necrosis, and neutrophilic inflammation, but again, no changes that the attending board-certified veterinary pathologists at our institution could attribute specifically to GRID irradiation. The remaining 4 dogs had stable disease (per RECIST) 6 weeks post-GRID. Acute RTOG grade I skin toxicity was observed in 3 of the 6 dogs, with 2 of those 3 having received 25 Gy. This included focal alopecia and hyperpigmentation (Figure 5). Subject 2 was euthanized 9 months after GRID, due to progressive weakness, lethargy, tumor-associated pain, and increased respiratory effort. Autopsy confirmed a high-grade STS with pulmonary metastasis. The primary tumor was composed predominately of necrotic tissue, with only a few regions of intact neoplastic cells captured in histologic section. Again, no changes were clearly associated with GRID irradiation; necrosis and inflammation are both characteristic of canine STS. Subject 4 was euthanized by the primary care veterinarian due to poor quality of life, 1 year after GRID irradiation. Autopsy was not pursued, and no description of the tumor was provided. Subject 5 was euthanized 3 months after GRID irradiation by the primary care veterinarian. The tumor had become ulcerated since the end of the study period; autopsy was not pursued. Subject 6 was alive at the time of manuscript preparation; the tumor remains intact but has reportedly progressively grown since the end of the study period (per the family).

Similar to human tumors treated with GRID, in the absence of measurable reduction in tumor size, there is no spike in S-SMase activity. Serum biomarkers (VEGF and TNF- $\alpha$ ) were quantified in all 6 dogs, immediately before GRID therapy and 1, 4, 24, and 48 hours later; due to a lab-handling error, S-SMase activity was assayed in only 5 of the 6 dogs (2 that were treated with 20 Gy and 3 that were treated with 25 Gy). With such a small study size, and

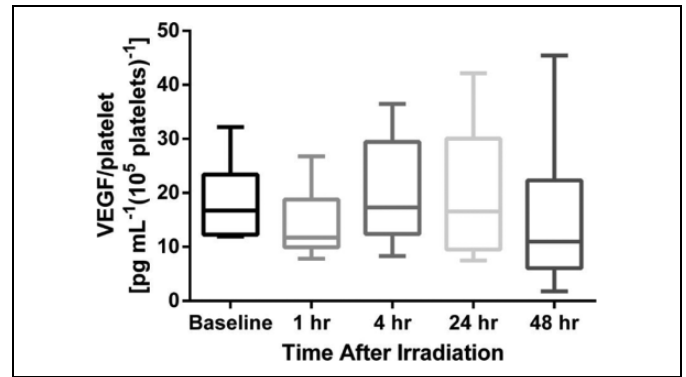


**Figure 6.** Platelet-corrected concentration of vascular endothelial growth factor (VEGF) as a function of time after irradiation, depicted using a box and whisker plot.

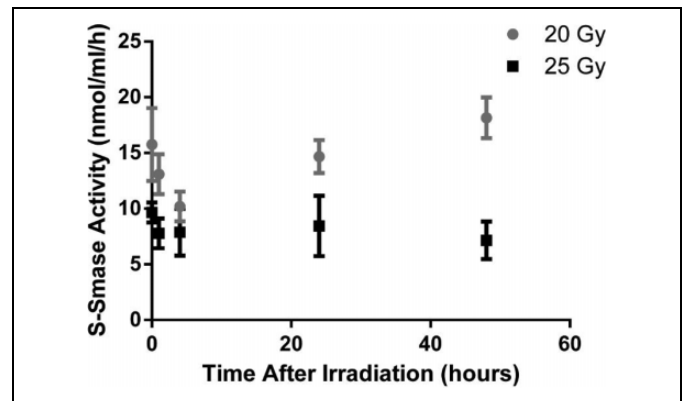


**Figure 7.** Secretory sphingomyelinase (S-SMase) activity as a function of time after irradiation; error bars depict the standard deviation of the mean.

**Table 3.** Serum Concentration of Tumor Necrosis Factor  $\alpha$  (pg/mL), as a Function of Time After Irradiation.

GRID Dose	Subject ID	TNF- $\alpha$ (pg/mL)				
		Pre-GRID	1 hour	4 hours	24 hours	48 hours
20 Gy	1	0.38	0	0	0	0
	2	0	0	0	0	0
	3	0	0	0	0	0
25 Gy	4	2.42	0	0	0	0
	5	1.71	0.08	0	0	0
	6	0.8	0	0	0	0

Abbreviation: TNF, tumor necrosis factor.

without appropriate control populations, it is difficult to ascribe significant meaning to results of statistical tests. Therefore, a combination of statistical results and qualitative descriptions of data is provided. Data are summarized in Figures 6, 7, and Table 3.

Although not meeting statistical significance ( $P < .05$ ) in a Friedman test, the platelet-corrected VEGF concentration decreased below baseline in 5 of the 6 subjects, 1 and 48 hours

after GRID irradiation, suggesting a trend toward a treatment-induced decline in VEGF.

The only statistically significant change was a decrease in S-SMase activity 48 hours after 25 Gy GRID ( $P = .03$  in a Friedman test). The S-SMase activity decreased from baseline in 4 of 5 subjects, at 1 hour post-GRID. Values returned to, or were higher than, baseline in 3 subjects by the 24-hour time point. To aid in interpretation of S-SMase assay results, TNF- $\alpha$  was also quantified in serum and was measurable at baseline in 4 of the 6 dogs and decreased (or was below the lower detection limit) in each of those subjects at all post-GRID time points.

## Discussion

This work documents that these GRID therapy protocols are generally well tolerated with regard to acute radiation toxicity in dogs and that GRID therapy alone is of no apparent use in palliating canine patients with STS. GRID has biologic activity similar to that experienced by human patients with cancer, in that GRID monotherapy does not induce measurable tumor shrinkage. Our study suggests that GRID treatment may modulate canine tumor vasculature, as indicated by apparent changes in serum concentrations of VEGF. Thus, results of this study demonstrate the feasibility of clinical implementation of a GRID therapy program in a veterinary radiation oncology clinic for the purposes of performing comparative oncology research. Furthermore, although the study period ended 6 weeks after GRID irradiation, surgical and/or postmortem histopathologic descriptions of the tumors were available for half of the enrolled subjects. Although this was a small study, it does demonstrate that the ability to successfully acquire autopsy data for a relatively high proportion of enrolled subjects is a strength of canine comparative oncology studies.

This study was exploratory in nature and was limited by small sample size and lack of a control population (either unirradiated negative controls or positive controls having received conformal RT). Despite these limitations, the data indicate that the pet dogs with spontaneously arising tumors may be a good model for translational research of SFRT. We observed that there was no temporal rise in S-SMase activity in these dogs that did not respond to GRID therapy. This is similar to what has previously been reported in humans, when bulky tumors are treated with GRID, wherein a rise in S-SMase coincided with tumor shrinkage, but ceramide and S-SMase activity was unchanged in patients whose tumors did not shrink.<sup>17</sup> This observation must be made with caution, though, because we do not know if a GRID-responsive canine tumor would have the same S-SMase response as is seen in humans, as none of the dogs in this study had a measurable tumor volume reduction after GRID irradiation. Furthermore, because there are no known reports of single fraction GRID irradiation (without additional chemoradiotherapy) for human sarcomas, we cannot comment as to whether the lack of measurable volume reduction in canine STS is consistent with the clinical outcome expected in people.

Similar to what has been described in serum samples from human patients with cancer before GRID irradiation, the dogs in this series had highly variable basal levels of S-SMase activity. This may be due to variations in interindividual differences in low-density lipoprotein content (not quantified) and/or presence of systemic inflammation before treatment.<sup>17</sup> It is difficult to explain the apparent decrease in S-SMase activity in the hours after GRID. It is possible that the radiation kills many endothelial cells and macrophages (these 2 cell types are the main source of the secretory SMase) and we see a drop simply because there are far fewer cells that produce it (even though secretion per cell might be stimulated). It is interesting that at 20 Gy (but not at 25 Gy), S-SMase activity start increasing after 24 hours, which might be due to the fact that radiation damage at 20 Gy was less pronounced than at 25 Gy, and thus stimulation may be observed after recovery of the macrophage/endothelial population. It was also hypothesized, since the activity is normalized per milliliter of sample, that the S-SMase activity could be artificially decreased due to dilution of blood during radiotherapy. In fact, dogs do receive IV fluid therapy during irradiation. That said, the total volume of IV fluids administered represented as a percentage of total estimated blood volume ranged from 3.1% to 7.7%, administered over 45 to 90 minutes. This does not seem like a large enough dilution to account for the activity changes observed in individual dogs. Finally, secretion of S-SMase in response to GRID is likely mediated by TNF- $\alpha$ , so an observed initial decrease in canine S-SMase activity might reflect slower TNF- $\alpha$  secretion in dogs than humans. The fact that TNF- $\alpha$  was measurable in some dogs before GRID, but became unmeasurable (results below the detection limit) after GRID, is an interesting trend that might account for the initial observed drop in sphingomyelinase activity, though confirmatory studies would certainly be needed to support that hypothesis. Ionizing radiation is known to induce the expression of TNF- $\alpha$ , which is a pro-inflammatory cytokine. In human patients treated with GRID, measurable increases in serum concentrations of this cytokine are common in tumors for which a complete clinical response is noted, but serum levels remain stable, or even decrease, in patients who do not experience a measurable response. Therefore, the lack of TNF- $\alpha$  induction in our canine population is not surprising, and the decrease is not unprecedented. In fact, the failure to induce this cytokine could possibly explain the lack of observable clinical response. Another possibility is that because TNF- $\alpha$  is relatively difficult to detect at low concentrations, the local change was not strong enough to result in a measurable increase in serum concentrations.<sup>16</sup>

The potential that the observed changes in VEGF and S-SMase could be related to anesthesia should not be overlooked. Without a control group that received anesthesia alone, this study can make no conclusions in that regard. It should also be noted that this pilot study was designed with consideration of previously published data, wherein Sathishkumar and colleagues measured serum SMase activity and ceramide concentration before treatment and 24, 48, and 72 hours after GRID irradiation.<sup>17</sup> In this study, we omitted the 72-hour time point

but added 2 earlier points (1 and 4 hours). This was based on preclinical data suggesting that radiation-induced ceramide-mediated vascular endothelial apoptosis occurs within hours of radiation exposure.<sup>35</sup> Future studies to clarify our findings should include more measurement time points.

In summary, the new information generated by this study includes the observation that high-dose, single fraction application of GRID does not induce measurable reduction in volume of canine STS. Furthermore, and in contrast to previously published data, there was a trend toward short-term reduction in serum concentration of VEGF and serum activity of S-Smase. These observations should be verified, and the cause should be investigated. Because GRID can be applied safely, and because these tumors can be subsequently surgically resected as a component of routine veterinary care, pet dogs with sarcomas are an appealing model for studying the radiobiologic responses to SFRT.

Because any number of imaging and physiology assays could be performed *in vivo* before and after GRID application, and because the resected tumor would provide large volumes of tissue to evaluate any number of biological changes (eg, immune cell infiltrates, neoangiogenesis, phenotypic changes in cells within and outside the GRID pattern, etc), this “model” system should prove useful for investigators interested in studying more clinically relevant radiobiological effects of SFRT that cannot be easily or realistically recapitulated in existing rodent models or using existing mini- and microbeam technologies.

### Authors' Note

The senior authors, Michael W. Nolan and Sha Chang, contributed equally to this work.

### Acknowledgments

The authors thank Drs Gabriela Seiler and M. Keara Boss for guidance in study design, members of the NC State Clinical Studies Core, members of the NC State Radiation Oncology Service, as well as Drs Matthew Arkans, Krista Kelsey, and J. Armando Villamil for their assistance with clinical management of enrolled study subjects and Ms Danielle LaVine, Karen Marcus, and Tracy Parker for their technical assistance and contribution to data analysis.

### Declaration of Conflicting Interests

The author(s) declared no potential conflicts of interest with respect to the research, authorship, and/or publication of this article.

### Funding

The author(s) disclosed receipt of the following financial support for the research, authorship, and/or publication of this article: Financial support for this work was provided, in part, by the Didi Cancer Research Fund and a National Institutes of Health grant, 2R01AG019233.

### References

- Kohler H. Rontgentiefen therapie mit massendosen [in German]. *MMW*. 1909;56:2314-2316.
- Marks H. Clinical experience with irradiation through a GRID. *Radiology*. 1952;58(3):338-342.
- Liberson F. Value of multiperforated screen in deep x-ray therapy. *Radiology*. 1933;20(3):186-195.
- Mohiuddin M, Curtis DL, Grizos WT, Komarnicky L. Palliative treatment of advanced cancer using multiple nonconfluent pencil beam radiation—a pilot study. *Cancer*. 1990;66(1):114-118.
- Mohiuddin M, Fujita M, Regine WF, Megooni AS, Ibbott GS, Ahmed MM. High-dose spatially-fractionated radiation (GRID): a new paradigm in the management of advanced cancers. *Int J Radiat Oncol Biol Phys*. 1999;45(3):721-727.
- Penagaricano JA, Moros EG, Ratanatharathorn V, Yan Y, Corry P. Evaluation of spatially fractionated radiotherapy (GRID) and definitive chemoradiotherapy with curative intent for locally advanced squamous cell carcinoma of the head and neck: initial response rates and toxicity. *Int J Radiat Oncol Biol Phys*. 2010;76(5):1369-1375.
- Dilmanian FA, Morris GM, Zhong N, et al. Murine EMT-6 carcinoma: high therapeutic efficacy of microbeam radiation therapy. *Radiat Res*. 2003;159(5):632-641.
- Dilmanian FA, Qu Y, Feinendegen LE, et al. Tissue-sparing effect of x-ray microplanar beams particularly in the CNS: is a bystander effect involved? *Exp Hematol*. 2007;35(4 suppl):69-77.
- Dewhirst M, Fontanella A, Palmer G, et al. Vascular response to microbeam radiation therapy *in vivo* using a murine window chamber tumor model. *Med Phys*. 2012;39(6):3983-3983.
- Yuan H, Zhang L, Frank JE, et al. Treating brain tumor with microbeam radiation generated by a compact carbon-nanotube-based irradiator: initial radiation efficacy study. *Radiat Res*. 2015;184(3):322-333.
- Kanagavelu S, Gupta S, Wu X, et al. *In vivo* effects of lattice radiation therapy on local and distant lung cancer: potential role of immunomodulation. *Radiat Res*. 2014;182(2):149-162.
- Fontanella AN, Boss MK, Hadsell M, et al. Effects of high-dose microbeam irradiation on tumor microvascular function and angiogenesis. *Radiat Res*. 2015;183(2):147-158.
- Pollack A, Abramowitz M, Bossart E, et al. Prostate cancer phase 1 Lattice Extreme Ablative Dose (LEAD) trial: feasibility and acute toxicity. *Int J Radiat Oncol Biol Phys*. 2014;90(1): S455.
- Blanco Suarez JM, Amendola BE, Perez N, Amendola M, Wu X. The use of lattice radiation therapy (LRT) in the treatment of bulky tumors: a case report of a large metastatic mixed Mullerian ovarian tumor. *Cureus*. 2015;7(11):e389.
- Prasanna A, Ahmed MM, Mohiuddin M, Coleman CN. Exploiting sensitization windows of opportunity in hyper and hypo-fractionated radiation therapy. *J Thorac Dis*. 2014;6(4): 287-302.
- Sathishkumar S, Dey S, Meigooni AS, et al. The impact of TNF-alpha induction on therapeutic efficacy following high dose spatially fractionated (GRID) radiation. *Technol Cancer Res Treat*. 2002;1(2):141-147.
- Sathishkumar S, Boyanovsky B, Karakashian AA, et al. Elevated sphingomyelinase activity and ceramide concentration in serum of patients undergoing high dose spatially fractionated radiation treatment—implications for endothelial apoptosis. *Cancer Biol Ther*. 2005;4(9):979-986.



18. Stancevic B, Varda-Bloom N, Cheng J, et al. Adenoviral transduction of human acid sphingomyelinase into neo-angiogenic endothelium radiosensitizes tumor cure. *PLoS One*. 2013;8(8):e69025.
19. Forrest LJ, Chun R, Adams WM, Cooley AJ, Vail DM. Post-operative radiotherapy for canine soft tissue sarcoma. *J Vet Intern Med*. 2000;14(6):578-582.
20. McChesney SL, Withrow SJ, Gillette EL, Powers BE, Dewhirst MW. Radiotherapy of soft tissue sarcomas in dogs. *J Am Vet Med Assoc*. 1989;194(1):60-63.
21. Thrall DE, Larue SM, Pruitt AF, Case B, Dewhirst MW. Changes in tumour oxygenation during fractionated hyperthermia and radiation therapy in spontaneous canine sarcomas. *Int J Hyperthermia*. 2006;22(5):365-373.
22. Lawrence J, Forrest L, Adams W, Vail D, Thamm D. Four-fraction radiation therapy for macroscopic soft tissue sarcomas in 16 dogs. *J Am Anim Hosp Assoc*. 2008;44(3):100-108.
23. Plavec T, Kessler M, Kandel B, Schwietzer A, Roleff S. Palliative radiotherapy as treatment for non-resectable soft tissue sarcomas in the dog—a report of 15 cases. *Vet Comp Oncol*. 2006;4(2):98-103.
24. McChesney SL, Gillette EL, Dewhirst MW, Withrow SJ. Influence of WR-2721 on radiation response of canine soft-tissue sarcomas. *Int J Radiat Oncol Biol Phys*. 1986;12(11):1957-1963.
25. Gillette SM, Dewhirst MW, Gillette EL, et al. Response of canine soft-tissue sarcomas to radiation or radiation plus hyperthermia—a randomized phase-ii study. *Int J Hyperthermia*. 1992;8(3):309-320.
26. Thrall DE, Prescott DM, Samulski TV, et al. Radiation plus local hyperthermia versus radiation plus the combination of local and whole-body hyperthermia in canine sarcomas. *Int J Radiat Oncol Biol Phys*. 1996;34(5):1087-1096.
27. Viglianti BL, Lora-Michiels M, Poulson JM, et al. Dynamic contrast-enhanced magnetic resonance imaging as a predictor of clinical outcome in canine spontaneous soft tissue sarcomas treated with thermoradiotherapy. *Clin Cancer Res*. 2009;15(15):4993-5001.
28. Chi JT, Thrall DE, Jiang C, et al. Comparison of genomics and functional imaging from canine sarcomas treated with thermoradiotherapy predicts therapeutic response and identifies combination therapeutics. *Clin Cancer Res*. 2011;17(8):2549-2560.
29. Thrall DE, Maccarini P, Stauffer P, et al. Thermal dose fractionation affects tumour physiological response. *Int J Hyperthermia*. 2012;28(5):431-440.
30. Buckey C, Stathakis S, Cashon K, et al. Evaluation of a commercially-available block for spatially fractionated radiation therapy. *J Appl Clin Med Phys*. 2010;11(3):2-11.
31. Cox JD, Stetz J, Pajak TF. Toxicity criteria of the Radiation Therapy Oncology Group (RTOG) and the European Organization for Research and Treatment of Cancer (EORTC). *Int J Radiat Oncol Biol Phys*. 1995;31(5):1341-1346.
32. LaDue T, Klein MK. Toxicity criteria of the veterinary radiation therapy oncology group. *Vet Radiol Ultrasound*. 2001;42(5):475-476.
33. Costelloe CMC, Chuang HH, Madewell JE, Ueno N. Cancer response criteria and bone metastases: RECIST 1.1, MDA and PERCIST. *Journal of Cancer*. 2010;1:80-92.
34. Nikolova-Karakashian M, Morgan ET, Alexander C, Liotta DC, Merrill AH, Jr. Bimodal regulation of ceramidase by interleukin-1beta. Implications for the regulation of cytochrome p450 2C11. *J Biol Chem*. 1997;272(30):18718-18724.
35. Garcia-Barros M, Lacorazza D, Petrie H, et al. Host acid sphingomyelinase regulates microvascular function not tumor immunity. *Cancer Res*. 2004;64(22):8285-8291.